

# Spectral properties of Dy<sup>3+</sup>-doped potassium niobate silicate glasses for white light emission

M. Murali Mohan<sup>1</sup>

**Abstract**— this paper reports on the preparation and characterization of different concentrations of Dy<sup>3+</sup>-doped potassium niobate silicate glasses (KNbSi). Raman spectrum was recorded to find the structural units in the present glass. The Judd- Ofelt (JO) theory has been used to determine the intensity parameters ( $\Omega_2$ ,  $\Omega_4$  and  $\Omega_6$ ) from the spectral intensities of absorption bands. The emission spectra revealed two sharp peaks at 485 nm (blue) and 577 nm (yellow) by the excitation with 378 nm radiations. The CIE co-ordinates (x, y) for different concentration of Dy<sup>3+</sup>- doped glasses were calculated along with the correlated color temperatures (CCT). In addition, the lifetimes of <sup>4</sup>F<sub>9/2</sub> level were measured by monitoring the <sup>4</sup>F<sub>9/2</sub> → <sup>6</sup>H<sub>15/2</sub> emission transition (486 nm). The decay times of the <sup>4</sup>F<sub>9/2</sub> level for different Dy<sup>3+</sup> ion concentrations are found to be single exponential at lower concentrations (≤ 0.5 mol %) and gradually changed to non-exponential for higher concentrations (≥ 1.0 mol %). The non-exponential nature of decay curves fitted to Inokuti-Hirayama model for S = 6, confirmed that the energy transfer between the excited Dy<sup>3+</sup> (donor) and unexcited Dy<sup>3+</sup> (acceptor) ions is of dipole-dipole type. From the magnitudes of yellow to blue (Y/B) intensity ratios, CIE chromaticity coordinates and correlated color temperatures (CCT) it is concluded that Dy<sup>3+</sup>-doped KNbSi glasses are potential for the development of white light emission.

**Index Terms**— Color coordinates, Dy<sup>3+</sup> ions, Decay rate, Emission spectra, Judd-Ofelt theory, Raman spectra

## 1 INTRODUCTION

Luminescence materials play an important functional role in many fields, such as lasers, solid state lighting, display screens, sensors and optical communications etc, [1-4]. In this technological aspect mostly, several rare earth (RE) doped crystalline and non-crystalline luminescent materials have been extensively studied [5-8]. Glasses activated with RE ions play significant role in the development of lasers, fiber amplifiers and white light emitting diodes (WLED), because of their relative features of easy preparation, shaping and doping flexibility of active ion concentrations. Generally, the luminescence efficiency of the RE ions mainly depends on energy transfer, excitation path, host material and phonon energy of host materials. Fluoride matrices possess low phonon energies and hence favorable for the enhancement of radiative transition rates and quantum efficiencies. But, fluoride matrices have poor glass forming ability, chemical durability and mechanical stability. In addition fluoride glasses are toxic, corrosive and also unstable for practical applications. Because of these reasons, conventional oxide glasses are preferred due to their wide applications in various fields such as optoelectronics, thermo chemical, nuclear and solar energy technologies [9-13]. Among different glass matrices, the silicate glasses possess low thermal expansion coefficient, low nonlinear refractive index, high surface damage threshold, large tensile fracture strength, easy fiber drawing ability and good chemical durability. Silica based optical fibers are widely used for telecommunications which operates at 0.8 $\mu$ m, 1.31 $\mu$ m and 1.55 $\mu$ m for first, second and third windows respectively [14 -17]. The addition of K<sub>2</sub>O and Nb<sub>2</sub>O<sub>5</sub> modifies the field strength of cations and to improve the mechanical strength which is prerequisite for a good laser glass [18].

In this paper spectral properties of Dy<sup>3+</sup> doped potassium niobate niobate silicate glasses were reported. Usually, Dy<sup>3+</sup> ions have two dominant emission bands one corresponding to <sup>4</sup>F<sub>9/2</sub> → <sup>6</sup>H<sub>13/2</sub> (yellow) and another corresponding to <sup>4</sup>F<sub>9/2</sub> → <sup>6</sup>H<sub>15/2</sub> transition (blue). Judd- Ofelt [19, 20] theory, analysis, concentration dependent emissions, excited state lifetimes, chromaticity color coordinates (x, y) and correlated color temperatures (CCT) evaluated from the emission spectra of Dy<sup>3+</sup>- ions doped in KNbSi glasses have been systematically analyzed and discussed.

- M. Murali Mohan presently pursuing Doctor of philosophy in Department of Physics, Sri Venkateswara University, Tirupati-517 502, India. PH-919000214138. E-mail: muralimohanster@gmail.com

## 2. Experimental details

### 2.1. Materials and methods

Dy<sup>3+</sup>- doped KNbSi glasses with a chemical composition of 30 K<sub>2</sub>O - 25 Nb<sub>2</sub>O<sub>5</sub> - (45- x) SiO<sub>2</sub> - x Dy<sub>2</sub>O<sub>3</sub> (KNbSiDy), where x = 0.05, 0.1, 0.5, 1.0 and 2.0 mol %, were prepared by conventional melt quenching technique which are referred as KNbSiDy005, KNbSiDy01, KNbSiDy05, KNbSiDy10 and KNbSiDy20, respectively. The starting materials of K<sub>2</sub>CO<sub>3</sub>, Nb<sub>2</sub>O<sub>5</sub>, SiO<sub>2</sub> and Dy<sub>2</sub>O<sub>3</sub> (99.9%) with the batch quantities of ~15 g were mixed and grinded in agate mortar. The homogeneous mixtures were taken in a platinum crucible and melted in electric furnace at 1350°C for about 3 hs. The melts were then poured onto a preheated brass mould at a temperature of 450°C and the glass samples were annealed for 12 hs to re-

move the thermal stress and strain.

## 2.2. Physical and spectral measurements

For the 1.0 mol % Dy<sup>3+</sup>-doped KNbSiDy10 glass, physical quantities such as density ( $d = 3.75 \text{ g cm}^{-3}$ ), concentration ( $C = 1.506 \times 10^{20} \text{ ions/cm}^3$ ) and the refractive index ( $n = 1.797$ ) were determined. The Raman spectrum of the undoped sample was measured by Renishaw inVia Raman microscope using 785 nm diode laser. The optical absorption spectrum of KNbSiDy10 glass was recorded on a Perkin Elmer Lambda-950 UV-Vis-NIR spectrophotometer in the wavelength range of 360-1900 nm. The emission and the decay measurements were done by exciting the samples at 387 nm using Jobin Yvon Fluorolog-3 spectrofluorimeter with xenon arc lamp as an excitation source.

## 3. RESULTS AND DISCUSSION

### 3.1. Analysis of Raman spectrum

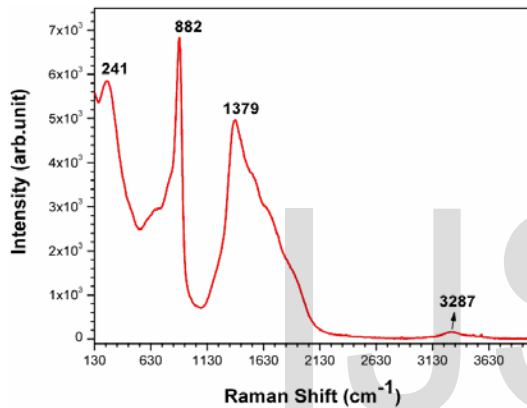


Fig.1. Raman spectrum of undoped KNbSi glass with 785 nm laser excitation

The undoped KNbSi glass has been studied using Raman spectroscopy. The unpolarized Raman scattering spectrum measured using the 785 nm laser excitation exhibits four bands centered at 241, 882, 1379 and 3281 cm<sup>-1</sup> as shown in Fig.1. It is noticed from Fig.1 that, the high intensity phonon band at 882 cm<sup>-1</sup> possesses lesser energy than that of pure SiO<sub>2</sub> glass, which has a maximum phonon band around 1100 cm<sup>-1</sup> [21]. The stretching modes of the Si-O-Si bands of SiO<sub>4</sub> tetrahedral with non-bridging oxygen atoms occur are active in the region 800-1300 cm<sup>-1</sup> [22, 23] and the stretching modes of the Nb-O bonds in the NbO<sub>6</sub> octahedral occur in the 300-900 cm<sup>-1</sup> region [24-26]. Particularly, the bands of SiO<sub>4</sub> occur at 1200, 1100, 950, 900, 850 cm<sup>-1</sup>, while for the Nb-O in octahedral symmetry occurs at 870, 730, 625, and 340 cm<sup>-1</sup>. The structural role of Nb<sub>2</sub>O<sub>5</sub> in silicate, borate, germanate and gallate glasses has been investigated and found that NbO<sub>6</sub> groups exist in the glass network [27, 28]. Fukumi et.al[26] investigated the structural position of NbO<sub>6</sub>- groups in K<sub>2</sub>O- Nb<sub>2</sub>O<sub>5</sub>- SiO<sub>2</sub> glass systems and noticed the Raman band in the 800- 900 cm<sup>-1</sup> region, which is attributed to NbO<sub>6</sub> octahedral with non-bridging oxygen and with much distortion. The broad bands in the 600-800 cm<sup>-1</sup> region are attributed to less distorted NbO<sub>6</sub> octa-

hedral without non-bridging oxygen's. The bands at 815- 870 cm<sup>-1</sup> are related to the Nb- O stretching modes of distorted NbO<sub>6</sub> octahedral sharing a corner with SiO<sub>4</sub> tetrahedral. As the Nb content increases, the NbO<sub>6</sub> octahedral as well as cluster start to appear, while the tetrahedral disappears. The characteristic intense band at 882 cm<sup>-1</sup> is attributed to the presence of Si- O-Si and the band at 241 cm<sup>-1</sup> is assigned to the presence of Nb-O. The characteristic bands around 1379 cm<sup>-1</sup> and 3281 cm<sup>-1</sup> are assigned to H- O- H vibrational mode.

### 3.2. Optical absorption

The observed optical absorption bands of Dy<sup>3+</sup> ions in the UV- VIS and NIR regions for KNbSiDy10 glass due to 4f-4f transitions are shown in Figs.2& 3, respectively. Eight absorption bands centered at 384, 424, 453, 473, 797, 892, 1086, 1256 and 1664 nm in the spectral range correspond to the <sup>6</sup>H<sub>15/2</sub> → <sup>4</sup>F<sub>7/2</sub>, <sup>4</sup>G<sub>11/2</sub>, <sup>4</sup>I<sub>15/2</sub>, <sup>6</sup>F<sub>5/2</sub>, <sup>6</sup>F<sub>7/2</sub>, <sup>6</sup>F<sub>9/2</sub>, <sup>6</sup>H<sub>9/2</sub> and <sup>6</sup>H<sub>11/2</sub> transitions, respectively. The assignments of the absorption transitions are done according to our earlier reported work [29]. The wavelengths of absorption bands along with their assignments are given in Table 1.

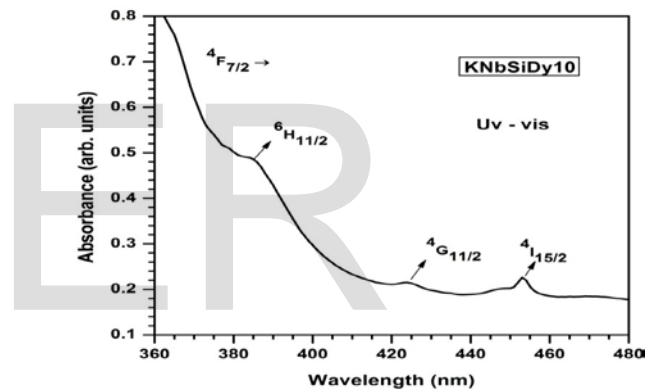


Fig. 2. Optical absorption spectrum of KNbSiDy10 glass for UV-Vis region

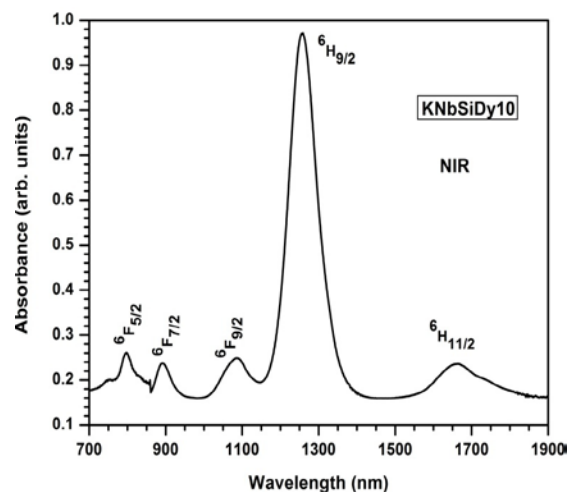


Fig. 3. Optical absorption spectrum of KNbSiDy10 glass for NIR region.

**Table 1:** Assignment of absorption transitions, peak positions ( $\lambda$ , nm) experimental ( $f_{exp}$ ) and calculated ( $f_{cal}$ ) oscillator strengths ( $\times 10^{-6}$ ) for KNbSiDy10 glass.

Transition ${}^6H_{15/2} \rightarrow$	Peak position ( $\lambda$ )	Oscillator strengths	
		$f_{exp}$	$f_{cal}$
${}^6H_{11/2}$	1664	1.32	1.47
${}^6H_{9/2}$	1256	9.12	9.69
${}^6F_{9/2}$	1086	2.73	2.57
${}^6F_{7/2}$	892	2.02	2.12
${}^6F_{5/2}$	797	1.66	1.35
${}^4I_{15/2}$	453	0.42	0.51
${}^4G_{11/2}$	424	0.17	0.11
${}^4F_{7/2}$	384	0.07	0.05

$\delta_{rms} = \pm 0.52$

### Judd-Ofelt analysis

The experimental oscillator ( $f_{exp}$ ) strengths of the absorption bands of  $Dy^{3+}$  ions in KNbSiDy10 glass are determined by measuring the integrated areas under the absorption bands. The Judd-Ofelt (JO) [19, 20] theory has been successfully used for the theoretical estimation of the intensities of the absorption bands of  $Dy^{3+}$  ions in KNbSiDy10 glass. This theory defines a set of three intensity parameters  $\Omega_\lambda$  ( $\lambda = 2, 4, 6$ ) which are dependent on host material. The JO parameters have been determined from the experimental oscillator strengths ( $f_{exp}$ ) using the least square fit method. From Table 1, it is noticed that there exists good agreement between experimental oscillator ( $f_{exp}$ ) and calculated oscillator ( $f_{cal}$ ) strengths with small rms value of  $\pm 0.52 \times 10^{-6}$ . From these JO parameters, important optical properties such as radiative transition probabilities for spontaneous emission, radiative lifetime of the excited states and branching ratios are calculated. In order to enhance the emission efficiency of a particular transition, the stimulated emission cross section ( $\sigma_e$ ) should be as large as possible. Hence it is therefore important to optimize the relation between the glass composition and the  $\Omega_\lambda$  parameters to obtain favorable spectroscopic properties for laser applications.

The evaluated JO parameters of  $Dy^{3+}$  ions in KNbSiDy10 are compared [30-33] in Table 2 and found that all the parameters follow the same trend as  $\Omega_2 > \Omega_4 > \Omega_6$ . It is well known that, the parameters of  $\Omega_4$  and  $\Omega_6$  values are related to the bulk properties, such as viscosity and rigidity of the glass and the magnitude of  $\Omega_2$  is indicates the covalent nature/structural changes in the vicinity of the  $Dy^{3+}$  ions [34]. The higher value of  $\Omega_2$  parameter indicates the more covalence between the  $Dy^{3+} - O^{2-}$  bands.

**Table 2:** Comparison of Judd-Ofelt parameters ( $\Omega_\lambda, \times 10^{-20} cm^2$ ) and their trends in different  $Dy^{3+}$ : doped glasses.

Glass	$\Omega_2$	$\Omega_6$	$\Omega_4$	Order
KNbSiDy10 [Present work]	10.26	2.03	2.38	$\Omega_2 > \Omega_4 > \Omega_6$
Oxyfluoride silicate glass[30]	2.69	1.64	1.64	$\Omega_2 > \Omega_4 = \Omega_6$
Fluoroborate[31]	2.90	0.98	1.09	$\Omega_2 > \Omega_4 > \Omega_6$
PKBAFDy10[32]	12.30	2.30	2.67	$\Omega_2 > \Omega_4 > \Omega_6$
Sodium zinc phosphate[33]	2.69	0.12	0.29	$\Omega_2 > \Omega_4 > \Omega_6$

### 3.4.

#### Emission spectra and radiative properties

Fig. 4 shows the visible emission spectra for different concentrations of  $Dy^{3+}$  doped KNbSi glasses under 387 nm excitation in the 430-700 nm region. The spectra consist two strong peaks in the blue (486 nm) and yellow (577 nm) regions and a weak band in the red region (666 nm) corresponding to the  ${}^4F_{9/2} \rightarrow {}^6H_{15/2}$ ,  ${}^4F_{9/2} \rightarrow {}^6H_{13/2}$  and  ${}^4F_{9/2} \rightarrow {}^6H_{11/2}$  transitions, respectively. The relative intensities of these bands can be varied by changing the excitation wavelength, host composition and  $Dy^{3+}$ -ion concentration. The  ${}^4F_{9/2} \rightarrow {}^6H_{15/2}$  transition is magnetic-dipole in nature, which hardly varies with the crystal-field strength of the host matrix, whereas the  ${}^4F_{9/2} \rightarrow {}^6H_{13/2}$  transition is hypersensitive ( $\Delta L = \pm 2$  and  $\Delta J = \pm 2$ ) and moreover, its intensity strongly depends on the host. Normally the  $Dy^{3+}$  ions are located lower symmetry and hence the yellow emission is more predominant. The emission intensities of all the three bands increase as the  $Dy^{3+}$  ions concentration increases from 0.05 to 1.0 mol % and then quenches at higher (>1.0 mol %) concentrations. The concentration quenching of emission intensity has been attributed to the migration of excited energy to the quenching centers (traps) or to the donors by the cross-relaxations process.

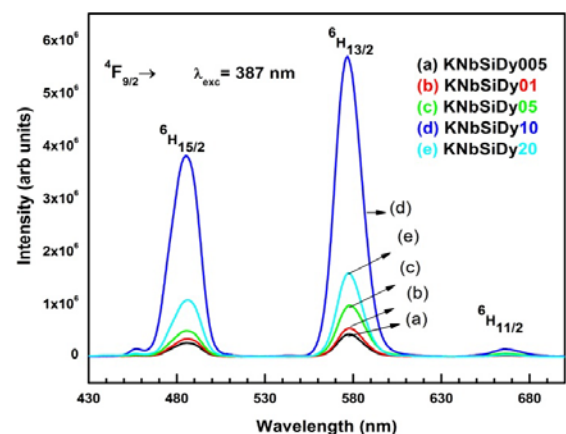


**Fig .4** Emission spectra for different concentration of  $Dy^{3+}$  ions in

*KNbSi glasses*

Radiative parameters such as emission band positions ( $\lambda_p$ , nm), effective bandwidths ( $\Delta\lambda_{eff}$ , nm), experimental branching ratios ( $\beta_{exp}$ ) and the peak stimulated cross-sections ( $\sigma_e(\lambda_p)$ ) of emission bands of  $Dy^{3+}$  ions in KNbSiDy10 glass are presented in Table 3.

**Table 3:** Emission peak positions ( $\lambda_p$ , nm), effective bandwidths ( $\Delta\lambda_{eff}$ , nm), radiative transition probabilities ( $A_R$ ,  $s^{-1}$ ), peak stimulated emission cross-sections ( $\sigma(\lambda_p)$ ,  $\times 10^{-21}$   $cm^2$ ), experimental ( $\beta_{exp}$ ) and calculated branching ratios ( $\beta_R$ ) of  $Dy^{3+}$

Transition $^4F_{9/2} \rightarrow$	$\lambda_p$	$\Delta\lambda_{eff}$	$A_R$	$\sigma$ ( $\lambda_p$ )	Branching ratios	
					$\beta_{exp}$	$\beta_R$
$^6H_{15/2}$	486	17.93	229	1.15	0.32	0.15
$^6H_{13/2}$	577	15.3	1359	5.78	0.59	0.64
$^6H_{11/2}$	666	16.2	160	0.98	0.03	0.05

ions in KNbSiDy10 glass.

**3.5. CIE Chromaticity coordinates and color purity**

The CIE [35] chromaticity diagram (Commission International de l'Eclairage 1931) is shown in Fig.5. The color coordinates calculated from emission spectra of different concentration of  $Dy^{3+}$ -doped KNbSi glasses are (0.35, 0.38), (0.34, 0.38), (0.36, 0.39), (0.36, 0.39) and (0.35, 0.39) for KNbSiDy0.05, KNbSiDy0.1, KNbSiDy0.5, KNbSiDy10 and KNbSiDy20 glasses, respectively. It is observed that all the chromaticity co-ordinates (x, y) fall in the white light region of CIE diagram.

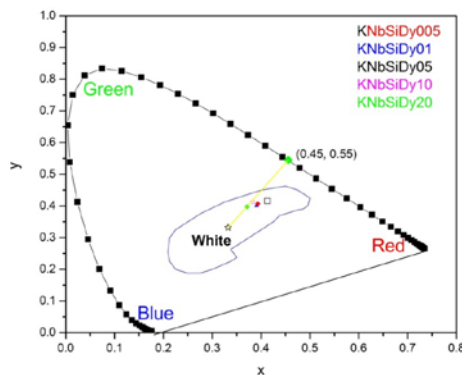


**Fig. 5** The CIE chromaticity diagram showing the color coordinates for different concentration of  $Dy^{3+}$  ions in KNbSi glasses.

The color purity of light source is defined as, the distance in the chromaticity diagram between the square root of emission color co-ordinates and co-ordinates of equal energy point, divided by the distance between the equal energy point and the dominant wavelength point which is indicated in Fig. 4. Thus, the color purity is given by

$$\text{Color purity} = \frac{\sqrt{(x - x_{ee})^2 + (y - y_{ee})^2}}{\sqrt{(x_d - x_{ee})^2 + (y_d - y_{ee})^2}} \quad (1)$$

where  $(x, y)$ ,  $(x_{ee}, y_{ee})$  and  $(x_d, y_d)$  are the chromaticity co-ordinates of the emitted light, equal energy point and the dominant wavelength points, respectively. To get the white light emission, the color purity of test source should be as low as possible. The color purity value of '0.15' calculated for the present KNbSiDy10 glass indicates that the titled glass can be considered as a suitable candidate for the white light emission.

**Table 4:** Yellow to blue (Y/B) intensity ratios and CIE chromaticity color coordinates for different concentrations of  $Dy^{3+}$  ions in KNbSi glasses.

Glass	Y/B ratio	Color coordinates		CCT (K)
		x	y	
KNbSiDy005	0.70	0.35	0.38	4923
KNbSiDy01	0.76	0.34	0.38	5251
KNbSiDy05	0.78	0.36	0.39	4656
KNbSiDy10	0.68	0.36	0.39	4656
KNbSiDy20	0.69	0.30	0.35	4955

The quality of light emitted by the light source can also be evaluated in terms of correlated color temperatures (CCT), which illustrates the temperature of a closest Planckian black-body radiator to the operating point in the chromaticity diagram [35]. The CCT values are calculated using the color coordinates by the McCamy empirical formula [36]

$$\text{CCT} = -449n^3 + 3525n^2 - 6823n + 5520.33 \quad (2)$$

where  $n = (x - x_e)/(y - y_e)$  is the inverse slope line and  $x_e = 0.332$ ,  $y_e = 0.186$  the epicenter. The CCT values obtained for the present titled glasses are in the range of 4923-4955K. Table 4 shows the values of Y/B ratios, color coordinates (x, y) and correlated temperature (CCT) for different concentrations of  $Dy^{3+}$  ions in KNbSiDy glasses.

**3. 6. Decay curves and lifetime measurements**

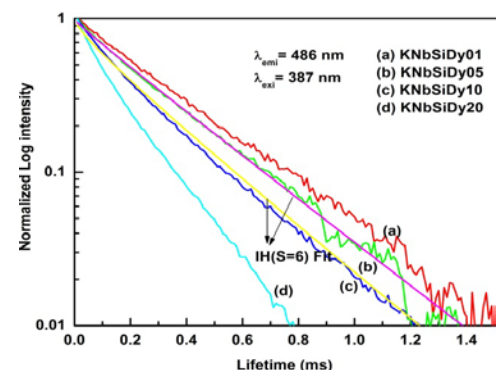


**Fig.6.** Decay profiles of  $^4F_{9/2}$  level for different concentration of  $Dy^{3+}$  ions in KNbSi glasses

various concentrations of  $Dy^{3+}$  ions. The measured lifetimes of  $^4F_{9/2}$  excited state determined are found to be 0.32, 0.35, 0.37, 0.29 and 0.24 ms for 0.05, 0.1, 0.5, 1.0, and 2.0 mol %  $Dy_2O_3$  doped glasses, respectively. The decay curves exhibited single exponential at lower  $Dy^{3+}$  ions concentrations ( $\leq$  up to 0.1 mol %) and turned into non-exponential nature at higher concentrations ( $\geq$  0.5 mol %) due to energy transfer between  $Dy^{3+}$  ions through cross-relaxation processes.

The theory of energy transfer process was first investigated by Forster [37] and Dexter [38]. Inokuti and Hirayama [39] modified the theory to account for ET between  $4f$  shells of trivalent  $RE^{3+}$  ions. They showed that the luminescence decay due to energy transfer can be described by the formula

$$I(t) = I_0 \exp \left[ -\frac{t}{\tau_0} - Q \left( \frac{t}{\tau_0} \right)^{3/S} \right] \quad (3)$$

where 't' is the time after excitation,  $\tau_0$  is the intrinsic decay time of the donors in the absence of acceptors. The ET parameter Q is defined as

$$Q = \frac{4\pi}{3} \Gamma \left( 1 - \frac{3}{S} \right) N_A R_0^3 \quad (4)$$

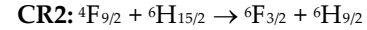
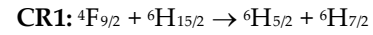
Q depends on S and the gamma function  $\Gamma(x)$ .  $\Gamma(x)$  is equal to 1.77 for dipole-dipole ( $S = 6$ ), 1.43 for dipole-quadrupole ( $S = 8$ ) and 1.3 for quadrupole-quadrupole ( $S = 10$ ) interactions.  $N_A$  is the acceptors concentration, which is almost equal to total concentration of RE ions, and  $R_0$  is the critical radius, defined as the donor-acceptor separation for which the rate of ET to the acceptors is equal to the rate of intrinsic decay of the donors. The dipole-dipole interaction parameter  $C_{DA}$  is related to  $R_0$  as

$$C_{DA} = \frac{(R_0)^S}{\tau_0} \quad (5)$$

The average distance between the donor and acceptor ions can be obtained from the following equation

$$R = \left( \frac{3}{4\pi C} \right)^{1/3} \quad (6)$$

The non-exponential nature of the decay curves are well-fitted to the Inokuti-Hirayama (IH) model [39] for  $S = 6$ , indicates that the energy transfer between the donor (excited ion) and the acceptor (ground state ion) ions is of dipole-dipole type. The energy transfer parameters (Q), donor-acceptor interaction parameters ( $C_{DA}$ ) and critical distances ( $R_0$ ) calculated from the IH models are presented in Table 5. The possible resonant cross-relaxation channels responsible for this energy transfer process are:



These cross-relaxation channels are indicated in the partial energy level diagram of Fig. 7 by the dotted arrows as CR1 and CR2, respectively.

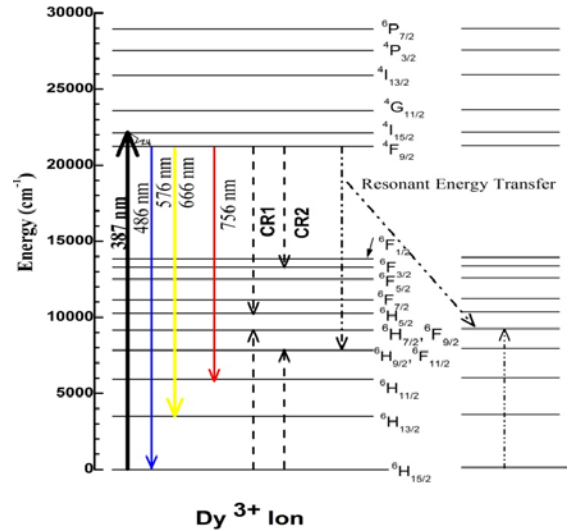


**Fig.7.** Partial energy level diagram showing the energy transfer cross-relaxation channels of  $Dy^{3+}$  ions in KNbSi glasses

#### 4. CONCLUSIONS

$Dy^{3+}$ - doped potassium niobate silicate glasses with chemical composition of  $30K_2O-25Nb_2O_5-(45-x)SiO_2-xDy_2O_3$  were prepared by the melt quenching technique and are characterized by the Raman, absorption, emission and lifetime measurements. The Raman spectrum revealed the basic structural units related to the presence of Si- O- Si and Nb- O bands which are attributed to  $NbO_6$  octahedral with non-bridging oxygens. The magnitudes evaluated JO parameters follow the order as  $\Omega_2 > \Omega_4 > \Omega_6$  and the higher value of  $\Omega_2$  for indicates the higher asymmetry around the  $Dy^{3+}$  ion in KNbSiDy glasses. The emission spectra exhibited two intense bands at 486 nm and 577 nm corresponding to  $^4F_{9/2} \rightarrow ^6H_{15/2}$  (blue) and  $^4F_{9/2} \rightarrow ^6H_{13/2}$  (yellow) transitions of  $Dy^{3+}$  ion, respectively. The luminescence intensity ratios (Y/B) were determined from the emission spectra of  $Dy^{3+}$  ions. The decay curves of  $^4F_{9/2}$  exhibited single-exponential at 0.05 mol% and turned to non-exponential at higher concentrations ( $\geq$  0.1 mol %). The decrease in fluorescence intensities as well as lifetimes at higher concentrations has been attributed to the energy transfer through cross-relaxation channels between the  $Dy^{3+}$  - ions.

#### References

- [1] E. Downing, L. Hesselink, J. Ralston, R. Macfarlane, Science 1996; 273: 1185-1189.
- [2] D. Lande, S. S. Orlov, L. Hesselink, R. R. Neurgaonkar, Opt. Lett. 1997; 22 : 1722-1774.

- [3] S. F. Colins, G. W. Baxter, S. A. Wade, T. Sun, K. T. V. Grattan, Z. Y. Zhang, A. M. Palmer, *J. Appl. Phys.* 1998; 84 : 4449-4654.
- [4] P. Xie, T. R. Gosnell, *Opt. Lett.* 1995; 20: 1014-1016.
- [5] W. Luo, R. Li, G. Lui, M. R. Antonio, X. Chen, *J. Phys.Chem. C* 2008; 112 (28):10370-10377.
- [6] P. Haro-Gonzalez, F. Lahoz, J. Gonzalez-Platas, J. M. Ca'ceres, S. Gonzalez-Perez, D. Marreno-Lo'pez, N. Capuj, I. R. Marti'n, *J. Lumin.* 2008; 128: 908-910.
- [7] P. Haro-Gonzalez, I. R. Marti'n, E. Arbelo-Jorge, S. Gonzalez-Perez, J. M. Ca'ceres, P. Nu'nez, *J. Appl. Phys.* 2008; 104 : 013112-013116.
- [8] P. Haro-Gonzalez, I. R. Marti'n, Albero Hernandez Creus, *Opt. Express* 2010 ; 18 (2) :582-590.
- [9] V. Rajendaran, N. Palanivelu, H. A. El-Batal, F. A. Khalifa, N. A. Shafi, *Acoust. Lett.* 1996; 23: 113-121.
- [10] H. Hirasimha, D. Arari, T. Yohida, *J. Amer. Ceram. Soc.* 1985; 68:486-489
- [11] Kanna, S. S Bhatti, K. J. Singh. K. S. Thind, *Nuclear Instru. Methods B* 1996; 114: 217-220.
- [12] K. Sing, H. Singh, V. Sharma, R. Naturam, A. Khanna, R. Kumar, H. S. Sahota, *Nuclear Instru. Methods B* 2002; 194: 1-6.
- [13] H. Singh, K. Sing, V. Sharma, R. Naturam, H. S. Sahota, *Nuclear Sci. Engg.* 2002 ; 142:342.
- [14] K. Wei, D. P.Machewirth, J. Wenzel, E. Snitzer, G. H. Sigel, *J. Opt. Lett.* 1994; 19: 904-906.
- [15] D. W. Hewak, B. N. Samson, J. A. Medeiros Neto, R. I. Laming, D. N.Payne, *Elect. Lett.* 1994; 30: 968-973.
- [16] S. Tanable, T. Hanada, M. Watane, T. Hayashi, N. Soga, *J. Am. Ceram. Soc.* 1995; 78: 2917-2922.
- [17] J. Heo, Y. B. Shin, *J. Non. Cryst. Solids* 1996; 196: 162-167.
- [18] J. H. Campbell, T. I. Suratwala, *J. Non-Cryst. Solids* 2000; 263&264: 318-341.
- [19] B. R. Judd, *Phys. Rev.* 1962; 127: 750-761.
- [20] G. S. Ofelt, *J. Chem. Phys.* 1962; 37: 511-520.
- [21] J. S. Wang , E. M. Vogel, E. Suitzer, *Opt. Mater.* 1994; 3:187-203.
- [22] W. L. Konijnendijk, *Glastechn. Ber.* 1975; 48: 216-222.
- [23] Y. Tsunawaki, N. Iwamoto, T. Hattori, A. Mitsuishi, *J. Non-Cryst. Solids* 1981; 44: 369-378.
- [24] Z. Wang, B. Sui, S. Wang, H. Liu, *J. Non- Cryst. Solids* 1986; 80: 160-166.
- [25] G. E. Rachkovkaya, N. M.Bobkova, *J. Non-Cryst. Solids* 1987; 90: 617- 620.
- [26] K. Fukumi, S. Sakka, *J. Mater. Sci. Letters* 1988; 23: 2819-2825.
- [27] Shtin and V. Mamochin, *Fiz. Khim. Stekla* 1982; 8: 170-178.
- [28] V. Kolobkov, E. Kolobkova, I. Mararov, V. Mamoshin, *Fiz. Khim. Stekla* 1986; 1: 352-359.
- [29] J. Suresh Kumar, K. Pavani, A. Mohan Babu, G. Neeraj Kumar, S.B. Rai, L. Rama Moorthy, *J. Lumin.* 2010; 130 : 1916-1923.
- [30] Z. Duan, J. Zhang, L. Hu; *J. Appl. Phys.* 2007;101: 043110-043117.
- [31] Y. Dwivedi, S.B. Rai, *Opt. Mater.* 2009; 31: 1472-1477.
- [32] R. Praveena, R. Vijaya, C.K. Jayasankar, *Spectrochimica. Acta PartA* 2008;70 :577-586.
- [33] G. Tripathi, V.K. Rai, S.B. Rai, *Spectrochimica. Acta Part A* 2005; 62:1120-1124.
- [34] C.K. Jorgensen, R.Reisfeld, *J. Less Common. Met.* 1983; 93: 107-112.
- [35] T. Erdem, S. Nizamoglu, X. W. Sun, H. V. Demir, *Opt.Express* 2010; 18(1) 340-347.
- [36] C. S. McCamy, *Color Res. Appl.* 1992; 17(2) : 142-144
- [37] T. Forster, *Ann. Physik* 1948; 6: 55-62.
- [38] D. Dexter, *J. Chem. Phys.* 1953; 21: 836-842.
- [39] M. Inokuti, F. Hirayama, *J. Chem. Phys.* 1965; 43: 1978-1989.